



Calibration of Microwave Spectrometry Setup and FT - IR Measurements

Bachelorarbeit

PA 138.085 Projektarbeit
Elektrodynamik neuartiger optischer Materialien

unter der Leitung von
Univ.Prof. Dr.rer.nat. Andrei Pimenov und
Dr. Graeme Eoin Johnstone

E138 - Institut für Festkörperphysik

von

Böhm David
e1127498

October 16, 2014

Contents

Abstract	I
1 Introduction	1
2 Theoretical basics	2
2.1 Characteristic impedance	2
2.2 Scattering parameters	2
2.3 Basics of FT spectrometry	4
2.4 Interference on coplanar boards	6
2.5 Drude-Lorentz model	6
3 Microwave measurements	7
3.1 Introduction to microwave measurements	7
3.2 Calibration without transmission line	8
3.3 Calibration with transmission line	11
3.4 Measurement	12
3.5 Correction	14
3.6 Result	18
3.7 Checking experiments	18
3.8 Discussion	19
4 FT-IR Measurements	20
4.1 FT-IR setup	20
4.2 Calibration	21
4.3 Measurement	21
5 Discussion and Outlook	24
Acknowledgement	25
References	27

Abstract

The focus of this work lies on the calibration of our microwave spectrometry measurement setup and as well as a measurement in the infrared range with a Fourier transform infrared spectrometer.

Our microwave setup contains a sample holder which can't be easily calibrated with the network analyser. So we have to do the calibration without the analyser just with maths and a mathematics program. To do this calibration we need to know which disturbance can happen in the coaxial sample holder. These errors are well known from the high frequency technology. There is a model called „Scattering Parameter“ which describes all errors in a two port system like our transmission line. To calibrate our setup we need three reference or calibration measurements. These three measurements determine the scattering parameter for the setup to correct the taken sample measurements to useful data. Our sample material is Mylar (BoPET - Biaxially-oriented polyethylene terephthalate). Out of our reflectance measurements we are able to calculate the dielectric constant ϵ_r for the measured sample. The dielectric constant of Mylar does not vary with frequency. Our reference measurement with well known reflectance coefficients are an open circuit, a short circuited circuit and a Mylar sample with a calculated coefficient. We expect the dielectric constant to be exactly the same as what we used for the calculation.

The second part of the report will discuss the mathematical background of the Fourier transform spectrometer and some measurements. This part will treat the basic function of the spectrometer and how to calibrate it and how to make a measurement. The measured samples are MgO and NdGaO₃ and the taken data will also be fitted.

1 Introduction

We are interested in the interaction of electromagnetic radiation with matter[1]. A medium is characterized by its material parameters such as the dielectric constant and the conductivity. The theoretical description of the phenomena of the experimental results presented here are based on Maxwell's equations, the time dependent solution of Maxwell's equations leads to wave propagation. There are also optical constants which characterize the propagation and the dissipation of electromagnetic waves in the medium: the refractive index and the impedance.

There are many ways of measuring material parameters and discovering effects which are characteristic for the material. Here we will focus on microwave wave measurement techniques and on infrared Fourier transform(IR-FT) spectroscopy.

For the microwave measurement we use a network analyser, which operates from below $1kHz$ up to $3GHz$. Network analysers are combined driver/response test systems which measure the magnitude and phase characteristics of linear networks. The measurement is based on the comparison between the incident signal and the reflected or transmitted signal. The incident signal is always a sine wave. The description of the linear network behaviour is provided in the whole frequency domain. To take all effects into account, calibration measurements are required. For example the resistance of the coaxial line or the conductors cause those effects.

A IR-FT spectrometer is based on a Michelson's design of an interferometer. There a light beam is split into two parts which follow different paths. After being recombined the intensity of the light is a function of the relative difference in the path length. So we can see an interference pattern. With a function of delay δ the spectral distribution of the light can be recovered by Fourier transformation. New Fourier transform spectrometers operate often in the infrared spectral range ($10-10000cm^{-1}$).

2 Theoretical basics

In microwave engineering a transmission line is a special cable or other structure which is designed to carry radio frequencies. The frequency of the current is high enough its wave nature must be taken into account.

2.1 Characteristic impedance

The transmission line is terminated by the impedance Z_L and the characteristic impedance[2] of the transmission line is Z_0 . On the transmission line (Fig.: 1) two waves propagate, one towards the load and the other away from the load. The incident wave with the voltage V_+ and the current I_+ from the generator to the impedance and the reflected wave back to the generator with the voltage V_- and the current I_- .

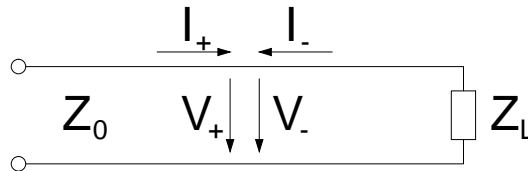


Figure 1: Model of voltage and current at a transmission line

The characteristic impedance is the ratio of voltage to current from a propagating wave. Since both waves propagate through the same transmission line, their voltages and currents are related

$$Z_0 = \frac{V_+}{I_+} = -\frac{V_-}{I_-} \quad (2.1)$$

The impedance Z_L is the ratio of the total voltage and current

$$Z_L = \frac{V}{I} = \frac{V_+ + V_-}{I_+ + I_-} \quad (2.2)$$

2.2 Scattering parameters

Up to frequencies of several megahertz networks can be calculated with the classical method of Kirchhoff's equations. The components of a network can't be described with easy equivalent circuits because of their parasitic elements and the correlation between them at higher frequencies. Our transmission line is such a component.

All voltages and currents (Fig.: 2) at the cable of the circuit have to be defined.

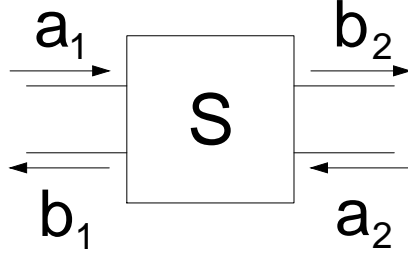


Figure 2: Two-Port system with wave quantities

Therefore the calculation is done with incident a_i and reflected b_i (with $i = 1, 2$) wave quantities and scattering matrix \mathbf{S} . Which is analogous to the dissection of the incident and reflected wave of voltage and current.

$$a_i = \frac{V_i + Z_i I_i}{2\sqrt{Z_L}} \quad (2.3)$$

$$b_i = \frac{V_i - Z_i I_i}{2\sqrt{Z_L}} \quad (2.4)$$

With $V = V_+ + V_-$ and $I = I_+ - I_-$. In general $\vec{b} = \mathbf{S} * \vec{a}$. The equation for a two-port network

$$\begin{pmatrix} b_1 \\ b_2 \end{pmatrix} = \begin{pmatrix} S_{11} & S_{12} \\ S_{21} & S_{22} \end{pmatrix} * \begin{pmatrix} a_1 \\ a_2 \end{pmatrix} \quad (2.5)$$

S_{11} is the reflection coefficient at port 1 if port 2 has no reflection. S_{22} is the reflection coefficient at port 2 if port 1 has no reflection. S_{12} describes the transmitted wave on port 1 if we apply a wave at port 2. The first index describes the port of the reflected wave and the second index describes the port where the wave is applied.

$$b_1 = S_{11}a_1 + S_{12}a_2 \quad (2.6)$$

$$b_2 = S_{21}a_1 + S_{22}a_2 \quad (2.7)$$

$S_{11} = S_{22}$ and $S_{12} = S_{21}$ applies for all symmetric two-ports. Now using the equations (2.1) and (2.2) and the definition of the reflection coefficient $S_{11} = V_-/V_+$ results to

$$Z_L = \frac{V_+ + V_-}{V_+ - V_-} Z_0 = \frac{1 + S_{11}}{1 - S_{11}} Z_0 \quad (2.8)$$

Which is equivalent to

$$S_{11} = \frac{Z_L - Z_0}{Z_L + Z_0} \quad (2.9)$$

Using the definition from a plate capacitor $C = \epsilon_0 \epsilon_r A/d$, the complex impedance $Z = 1/i\omega C$, $\omega = 2\pi f$ and (2.8) we obtain the complex dielectric constant ϵ_r . The dielectric constant is related to the reflection coefficient S_{11} by

$$\epsilon_r = \frac{1 - S_{11}}{(1 + S_{11}) i 2\pi f C_0 Z_0} \quad (2.10)$$

where Z_0 is the characteristic impedance and f is the measuring frequency. The dimensions of the sample determine $C_0 = \epsilon_0 A/d$. A is the area and d is the thickness of the sample.

2.3 Basics of FT spectrometry

A simple diagram of a Michelson interferometer shown in figure 3 is useful for explaining the basics of principles of Fourier transform spectroscopy[1].

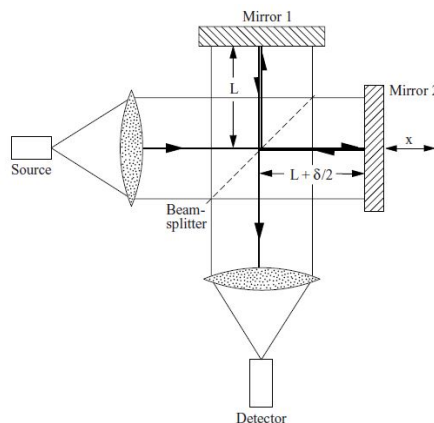


Figure 3: Michelson interferometer[1]

The frequency dependent spectrum $B(\omega)$ comes from an arbitrary source. The beam of the source is divided by the beamsplitter. One beam is directed to the fixed mirror 1 and the other beam is directed to the moving mirror 2. The distance from the beamsplitter to mirror 1 is L . If mirror 2 is moved to the distance $L \pm \delta/2$, the difference in path length is δ . If δ is a multiple of the wavelength ($\delta = n\lambda$ with $n = 1, 2, 3, \dots$) we observe constructive interference. If we have $\delta = (2n + 1)\lambda/2$ we see destructive interference. With the constructive part we get a light maximum and with destructive interference we detect no light. Hence the detector measures $I(\delta)$, the recombined beam intensity as a function of path difference. That means the we can convert the frequency dependence of the spectrum $B(\omega)$ into a spatial dependence of the recombined intensity $I(\delta)$. It is now possible to reconstruct $B(\omega)$ mathematically out of the spatial dependence intensity $I(\delta)$.

By using all mathematical background of Fourier transformation and applying it to the Michelson interferometer we can write the electrical field at the beam splitter as

$$E(x, \nu) d\nu = E_0(\nu) \exp\{i(2\pi x\nu - \omega t)\} d\nu \quad (2.11)$$

where $\nu = 1/\lambda = \omega/2\pi c$ is the wave number of the radiation. The beams have passed the beam splitter so one was reflected and one was transmitted. We consider that their amplitudes are equal. If the distance to travel is $2L$ for one light beam the other one has to travel the length $2L + \delta$. Then we can write the reconstructed field as

$$E_R(\delta, \nu) d\nu = \|\hat{r}\| \|\hat{t}\| E_0(\nu) [\exp\{i(4\pi L\nu - \omega t)\} + \exp\{i[2\pi(2L + \delta)\nu - \omega t]\}] d\nu \quad (2.12)$$

The beam splitter has the complex reflection and transmission coefficients \hat{r} and \hat{t} and we also have assumed that both beams have the same polarization. The intensity of a given spectral range is proportional to the square of the electric field ($E_R E_R^*$). Doing this step we obtain

$$I(\delta, \nu) d\nu \propto E_0^2(\nu) [1 + \cos(2\pi\nu\delta)] d\nu \quad (2.13)$$

If we integrate now over all wave numbers we obtain the total intensity form all wave numbers at a single path difference δ

$$I(\delta) \propto \int_0^\infty E_0^2(\nu) [1 + \cos(2\pi\nu\delta)] d\nu \quad (2.14)$$

Usually it is written some different

$$\left[I(\delta) - \frac{1}{2}I(0) \right] \propto \int_0^\infty E_0^2(\nu) \cos(2\pi\nu\delta) d\nu \quad (2.15)$$

The intensity in the limit of infinite path difference for a broad band source $I(\infty)$ corresponds to the intensity of the incoherent radiation. This incoherent radiation is exactly half the intensity obtained at equal paths $I(\infty) = I(0)/2$. The interferogram is actually the departure from the value of infinite path difference. With the fact that $B(\nu) \approx E_0^2(\nu)$ and (2.15) we can write the inverse Fourier transformation to

$$B(\nu) \propto \int_0^\infty \left[I(\delta) - \frac{1}{2}I(0) \right] \cos(2\pi\nu\delta) d\delta \quad (2.16)$$

Thus we can measure $I(\delta)$ from the interferometer and theoretically it is a simple task to do the Fourier transformation to achieve $B(\omega)$, the spectrum of the signal.

2.4 Interference on coplanar boards

If a wave with the wavelength λ and at an angle α hits a transparent, coplanar board[3] with a refraction index n then something is reflected and the other part is transmitted. The transmitted wave is reflected on the backside of the board and after the exit of the board it is parallel to the first reflected wave. So the optical path difference Δs is with a thickness d of the board

$$\Delta s = \frac{2nd}{\cos \beta} - 2d \cos \beta \sin \alpha \quad (2.17)$$

With $\sin \alpha = n \sin \beta$, $\alpha \approx 0$ we get $\Delta s \approx 2dn$. Using all these formulas and the constructive part of the interference we obtain

$$m + \frac{1}{2} = \frac{2nd}{\lambda} \quad (2.18)$$

2.5 Drude-Lorentz model

To fit our received data we use the program RefFIT. RefFIT is designed to analyse optical spectra. It uses the Drude-Lorentz (DL) model[4] for the dielectric constant $\epsilon(\omega)$

$$\epsilon(\omega) = \epsilon_{\infty} + \sum_j \frac{\omega_{p,j}^2}{\omega_{o,j}^2 - \omega^2 - i\gamma_j \omega} \quad (2.19)$$

It describes the response of a set of harmonic damped oscillators. With ϵ_{∞} as the so called high-frequency dielectric constant, which represents the contribution of all oscillators at very high frequencies. $\omega_{o,j}$ is the eigenfrequency and determines the position of the j-th oscillator. $\omega_{p,j}$ is the plasma frequency and it is connected to the amplitude of the j-th peak and γ_j is the linewidth of j-th peak.

The reflectivity $R(\omega)$ is expressed via the dielectric function $\epsilon(\omega)$ according to Fresnel formula

$$R(\omega) = \left| \frac{1 - \sqrt{\epsilon(\omega)}}{1 + \sqrt{\epsilon(\omega)}} \right|^2 \quad (2.20)$$

3 Microwave measurements

3.1 Introduction to microwave measurements

Measurements are always measurements from the reflection coefficient M_{11} of the sample. For these measurements we use a network analyser from Agilent Technologies. Our measuring setup (Fig. 4) also contains a coaxial transmission line with a sample holder on top of it. This transmission line is required to perform the measurement in a cryostat, but that is not object of this work. The cable between the analyser and the transmission line should be as short as possible to avoid environmentally caused errors.

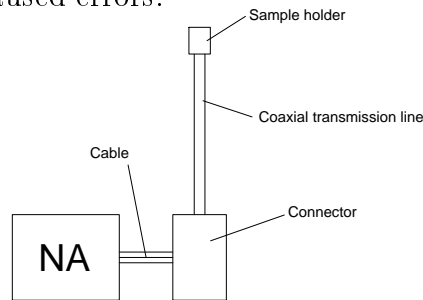


Figure 4: Schematic measuring setup

This transmission line is a coaxial air line which was built by Dr. Johnstone. The transmission line allows us to put the sample on top of it. Concerning the geometry of the sample holder (Fig. 5), samples with a diameter of $3mm$ or less and various thickness can be measured. We use a maximum diameter of $3mm$ because the inner part of the transmission line has the same diameter. The characteristic impedance of the transmission line $Z_0 = 50\Omega$ and the length is about $l = 95cm$.

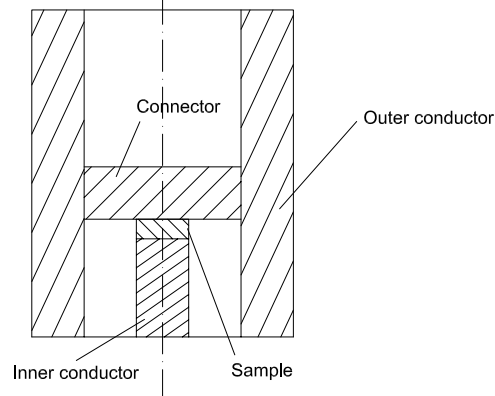


Figure 5: Schematic sample holder geometry

3.2 Calibration without transmission line

Before we can start the measurement, the network analyser needs to be calibrated. Such an option is integrated in the software of the analyser. You can only calibrate the equipment if it is standardised. That means, that we can only calibrate our setup (Fig.: 4) without the transmission line. Therefore we use appropriate commercial calibration standards.

Thus we choose the option „Calibration“ on our device, and apply one of the three standards to the setup. By choosing the „Open“ standard, the „Open“ button at the analyser must be pressed. This procedure must be repeated with the „Short“ and the „Load“ standard. In which „Open“ means an interrupted circuit, „Short“ means a short-circuited circuit. For the „Load“ a terminating impedance of 50Ω is used, which is equal to the characteristic impedance Z_0 of the analyser. Doing these three steps the scattering or error parameters explained in section 2.2 of this setup are determined. Those scattering parameters are complex numbers, so we obtain a real and an imaginary part. All measurements were taken in the frequency range between $3kHz$ and $3GHz$. The analyser is adjusted to take 601 data points in a logarithmic distribution.

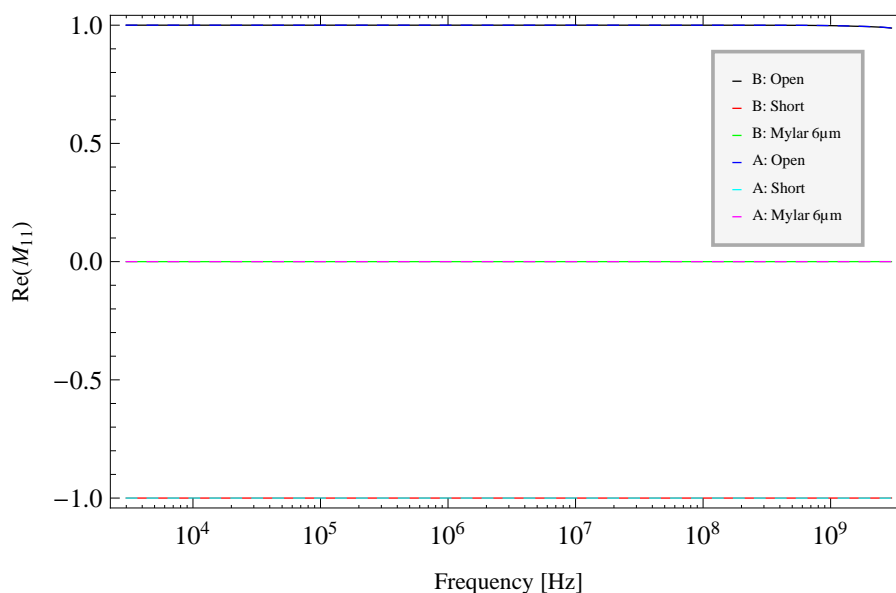


Figure 6: Real part measurement of the calibration, B: Before and A: After the actual measurement

Typically an open, a short and a matched load, with the reflection coefficients $S_{11,open} = 1$, $S_{11,short} = -1$ and $S_{11,load} = 0$ are chosen. With this choice the

absolute value is $|S_{11}| \leq 1$ and $S_{11,short} = -1$ means that the phase of the sine wave is shifted around 180° .

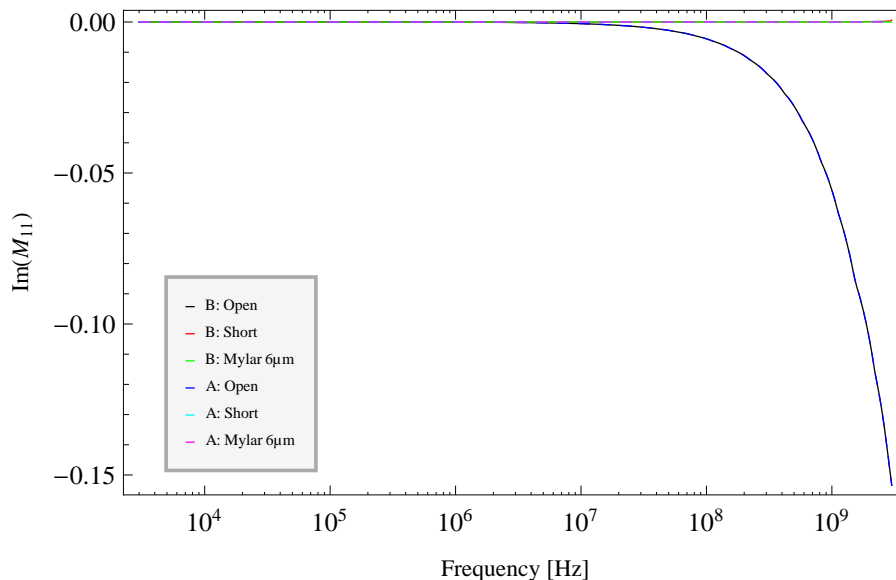


Figure 7: Imaginary part measurement of the calibration, B: Before and A: After the actual measurement

These two figures 6 and 7 are measured graphs of the calibration. We have also made an extra measurement before (B:) and after(A:) the actual one to ensure that the analyser works as we expect it to do.

In comparison to the calibration measurement we have taken another one with the same calibration and the connected transmission line. We have recorded these graphs 8 and 9 to make sure that the procedure is identical every time we perform it. Again we have performed the measurement twice. B means before and A after the actual measurement.

We see that in Fig.: 8 we have a slight difference in the A: Short line compared to the B: Short line. This difference may come from a little surface inaccuracy on the conductor of the sample holder. The next phenomena we can observe is the decrease of the signal at the frequency range above $100MHz$. We expect the signal to be almost as high as the appearing peak before because there should not be such high absorptions in this frequency range. We don't know why this happens, but maybe it's a product of a calibration which wasn't fully correct. This effect is observable in both plots (Fig. 8 and 9). Why this effect happens is a question that needs to be answered.

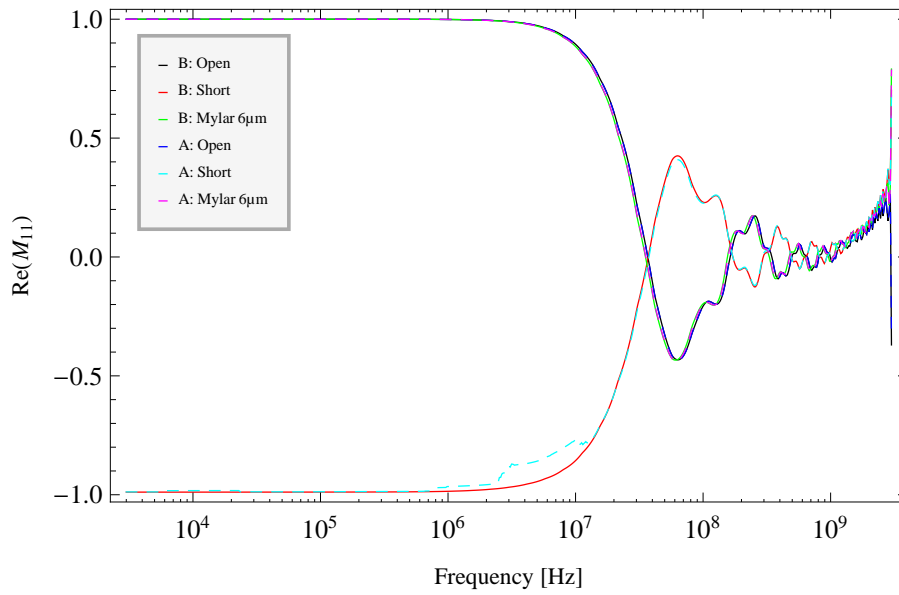


Figure 8: Real part measurement of the transmission line, B: Before and A: After the actual measurement

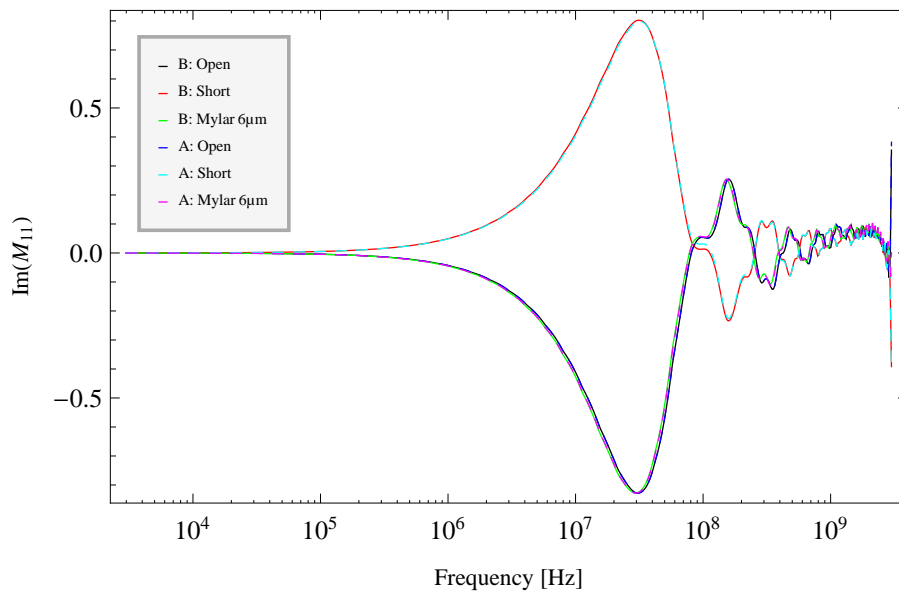


Figure 9: Imaginary part measurement of the transmission line, B: Before and A: After the actual measurement

3.3 Calibration with transmission line

After attaching the transmission line, the previous calibration is no longer valid. In microwave reflection measurement this transmission line is a source of errors. Mathematically this error source can be treated as a two port error network.

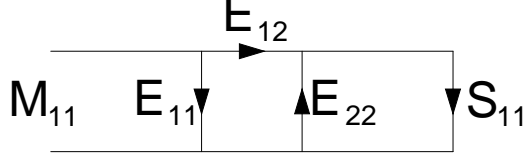


Figure 10: General error model

This figure 10 looks different to figure 2 but both describe the same problem. Here the E_i parameters are the same like the S_i in equation 2.5. $M_{11} = \frac{b_1}{a_1}$ is defined as measured reflection coefficient. $S_{11} = \frac{a_2}{b_2}$ is the real reflection coefficient of the sample.

Using the equations (2.6) and (2.7) we gain the measured reflection coefficient

$$M_{11} = E_{11} + \frac{E_{21}^2 S_{11}}{1 - S_{11} E_{22}} \quad (3.1)$$

This equation leads to the formula for the real reflection coefficient out of the measured coefficient as soon as the error coefficients are known

$$S_{11} = \frac{M_{11} - E_{11}}{E_{21}^2 + E_{22} (M_{11} - E_{11})} \quad (3.2)$$

Now it is clear that we need three calibration measurements to determine those error coefficients. In our case we have to do the calibration after the measurement with a calculation program. But we can't use the same reflection coefficient $S_{11,load} = 0$ for the load, because we don't have a sample which has an impedance of 50Ω in the whole frequency range. We have to use equation (2.9) for our load coefficient. For calibration we use a $6\mu m$ Mylar disc as load. So we have to calculate the $S_{11,load}$ for this mylar disc.

By solving (3.2) for each calculated coefficient $S_{11,i}$ with the computing software Mathematica we obtain the equations for the error coefficients

$$DE_{11} = S_{11,l} M_{11,o} M_{11,s} (S_{11,s} - S_{11,o}) + M_{11,l} M_{11,s} S_{11,o} (S_{11,l} - S_{11,s}) + \\ + M_{11,l} M_{11,o} S_{11,s} (S_{11,o} - S_{11,l}) \quad (3.3)$$

$$DE_{22} = M_{11,s} (S_{11,l} - S_{11,o}) + M_{11,l} (S_{11,o} - S_{11,s}) + M_{11,o} (S_{11,s} - S_{11,l}) \quad (3.4)$$

$$(DE_{21})^2 = (M_{11,l} - M_{11,o})(M_{11,l} - M_{11,s})(S_{11,l} - S_{11,o}) \\ (S_{11,l} - S_{11,s})(M_{11,o} - M_{11,s})(S_{11,o} - S_{11,s}) \quad (3.5)$$

D is the denominator of the equations (3.3), (3.4) and (3.5).

$$D = M_{11,l}S_{11,l}(S_{11,o} - S_{11,s}) + M_{11,s}S_{11,s}(S_{11,l} - S_{11,o}) + \\ + M_{11,o}S_{11,o}(S_{11,s} - S_{11,l}) \quad (3.6)$$

$M_{11,i}$ and $S_{11,i}$ are the measured reflectance and the calculated reflectance of the chosen reference samples. i stands for open, short and load.

With the parameters E_{11} , E_{21} and E_{22} we are able to convert the measured reflectance $M_{11,i}$ into the real reflectance $S_{11,i}$ of the sample. With i as a place holder for the chosen sample.

3.4 Measurement

We have made 3 measurements for calibration and we have also tried to measure two additional samples. Our choice fell on two Mylar samples with various thickness. The first one has a thickness of $15\mu m$ and the second one is $125\mu m$ thick. The reason why we have taken Mylar is that we could easily prepare samples of the correct thickness.

The measured reflection M_{11} is shown in the figures 11, 12 and 13.

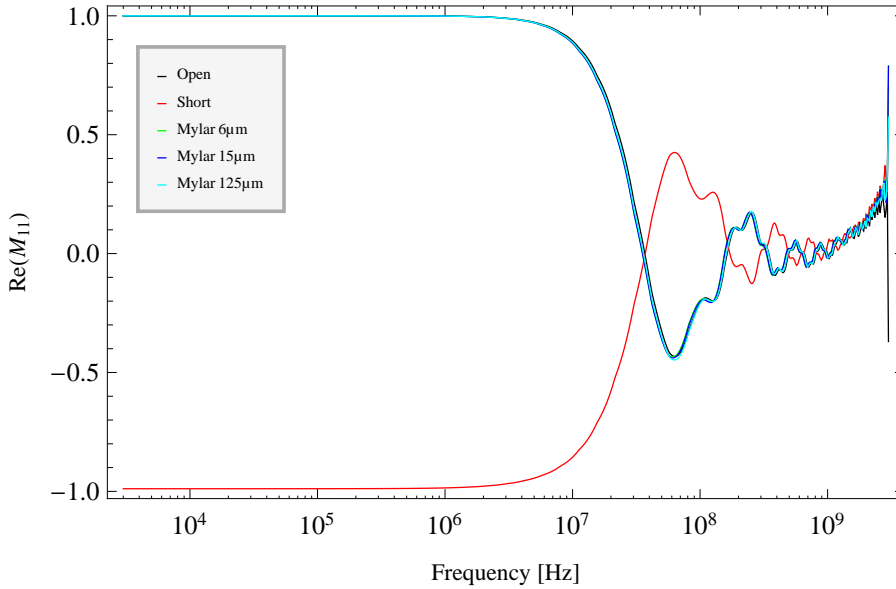


Figure 11: Real part of the measured data

One feature we can see in figure 11 and 13 before the correction is that the signal is decreased in the frequency range above 100MHz . This means that the absolute value of $|M_{11}|$ is very small in this frequency range. This is a feature which we don't expect.

We expect the samples to be close to the open signal at the beginning of the frequency range. At about 100MHz the sample matches the characteristic impedance of 50Ω . After this frequency the sample signals should get closer to the short signal. At a detailed look we can observe this feature already in the raw and uncorrected data (Fig.: 12). In the corrected plot it will be easier to detect.

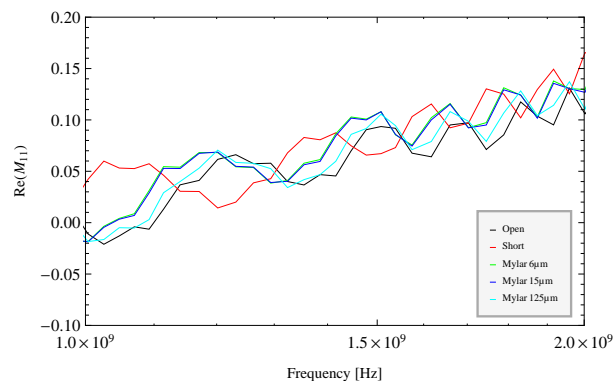


Figure 12: Detailed real part of the measured data

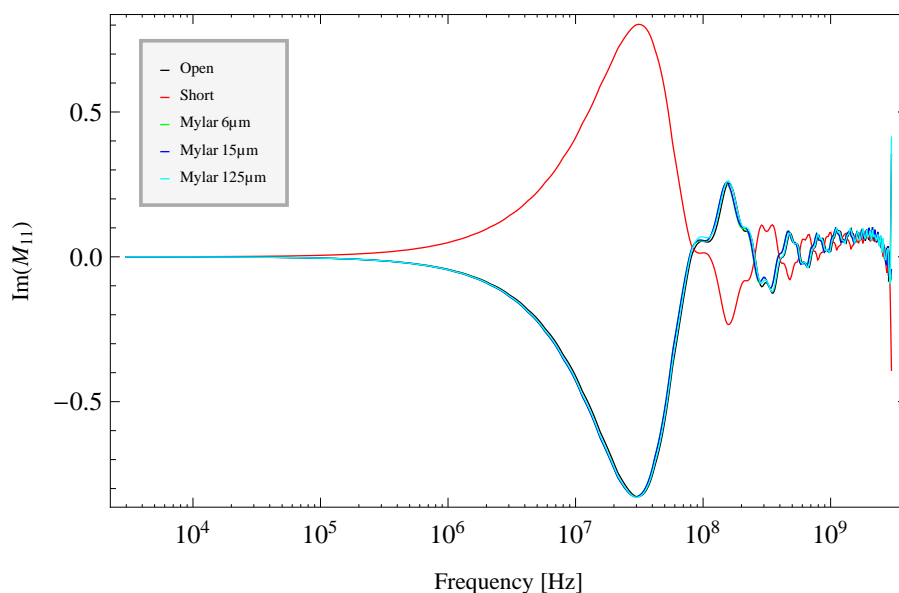


Figure 13: Imaginary part of the measured data

3.5 Correction

For calculating the error coefficients of the transmission line we have to use (3.3), (3.4) and (3.5). For $S_{11,open}$ we use $S_{11,open} = 1$ over the whole frequency range. For $S_{11,short}$ we use $S_{11,short} = -1$ over the whole frequency range. We use the Mylar with $6\mu m$ thickness as a load because it has an impedance as close as possible to 50Ω . The $S_{11,load}$ is calculated with (2.9). For $M_{11,i}$ we take the open, short and Mylar $6\mu m$ data shown in figure 11 and 13.

We get the following complex error coefficients (Fig.: 14 and 15).

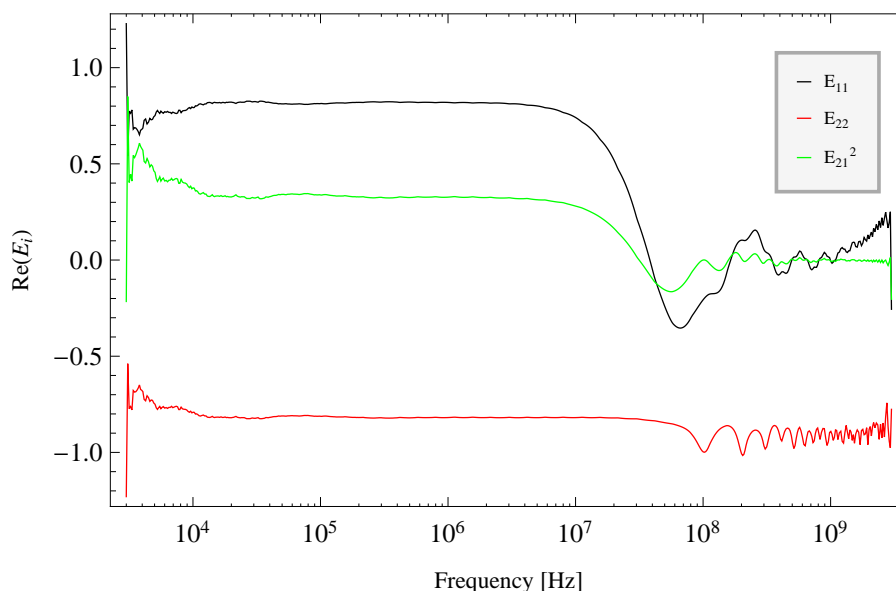


Figure 14: Real part of the calculated error coefficients

In figure 14 and 15 we can observe that the error parameters are connected to the features caused by the transmission line. They should compensate the features above a frequency of $100MHz$ shown in figure 11 and 13. One important point is that I have calculated the error parameter with two programs and I always got the same result. I did this to become clear that no program made a mistake.

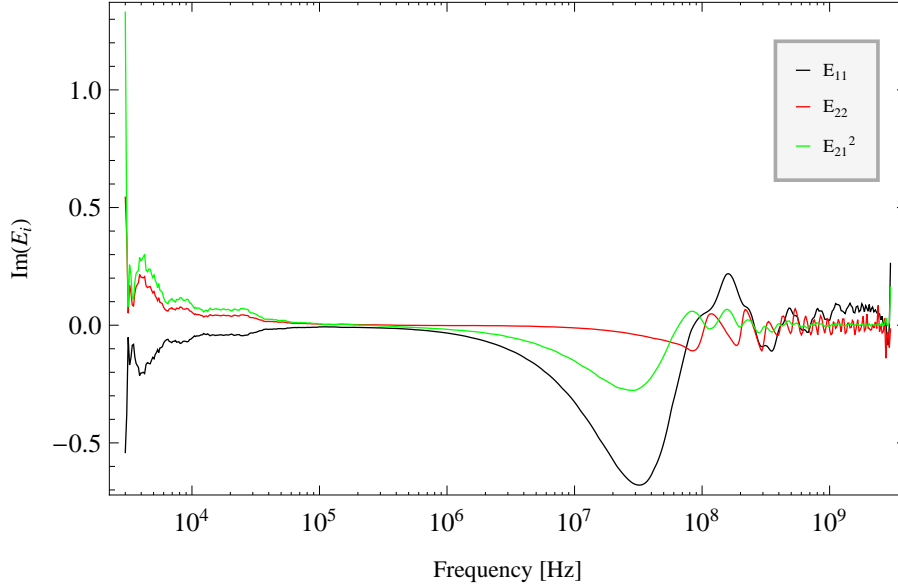


Figure 15: Imaginary part of the calculated error coefficients

By using (3.2) and the calculated error coefficients we can now correct the measurements. These corrections are shown in figure 16 and 17. Now all phenomena described before can be found in the plots 16 and 17. First of all the approach of all samples from the open to the short signal can be watched very easily. The next thing is that at about 100MHz something occurs. There are huge peaks in the corrected lines and they are somehow connected to the signal decrease above 100MHz in the raw measurements (Fig.: 11 and 13).

The dashed lines are the calculated S_{11} parameters of the samples in ascending order. The $6\mu\text{m}$ sample is our reference sample so it matches perfect to the calculated line, implying that the correction calculation works very well. In the case of the other two sample we can see something like a shift. They are shifted to the calculated line from the previous sample. The corrected sample data is in the range between the $6\mu\text{m}$ sample and their own calculated line. This shift is a sort of coincidental effect which is caused by a connected reason.

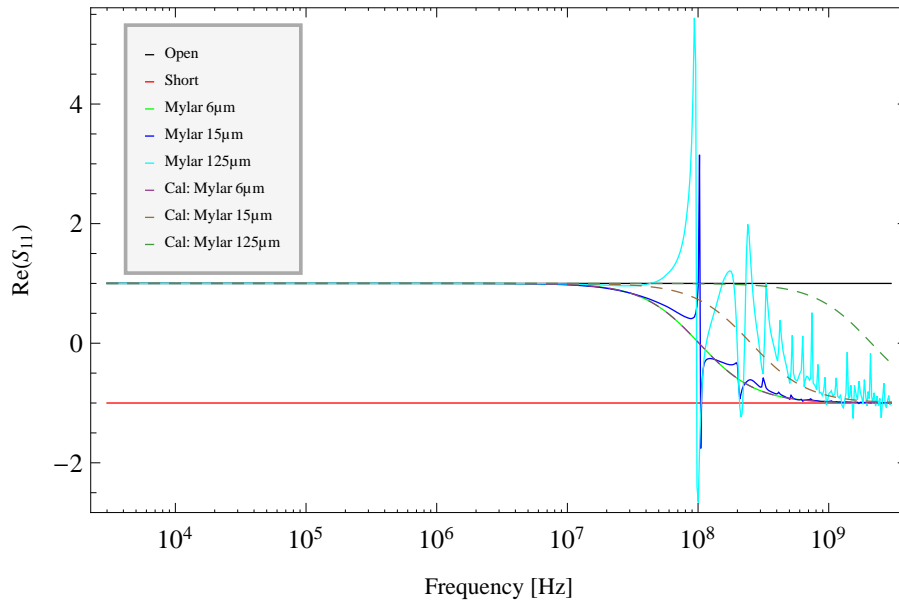


Figure 16: Real part of the corrected data

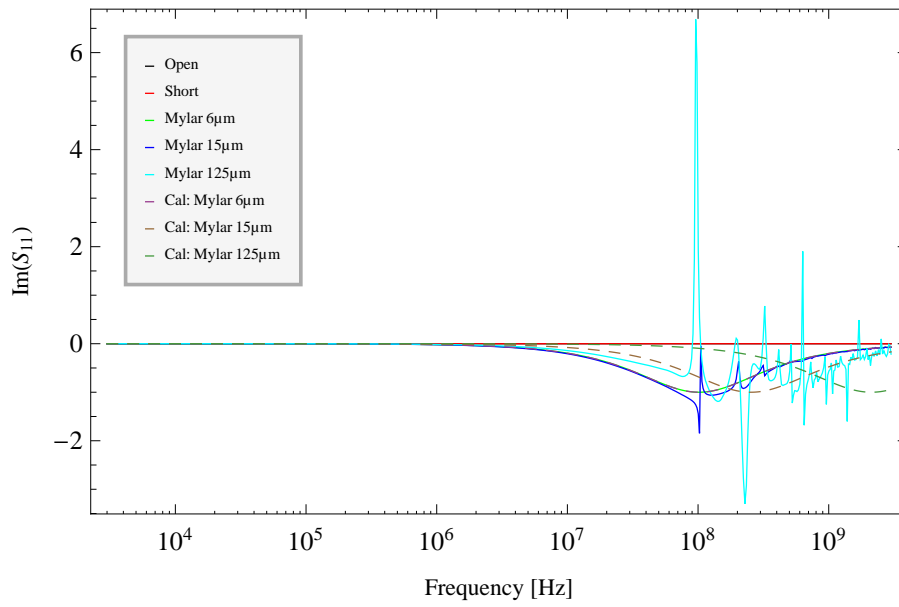


Figure 17: Imaginary part of the corrected data

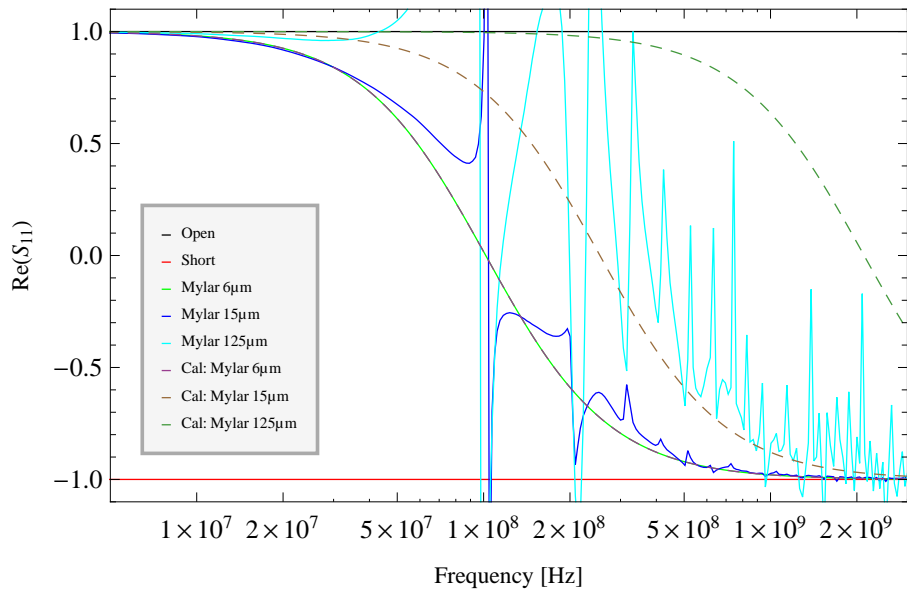


Figure 18: Real part of the corrected data in the frequency range $5 * 10^6 \text{ Hz}$ to $3 * 10^9 \text{ Hz}$ and $|S_{11}| \leq 1$ for a detailed look without irrelevant peaks

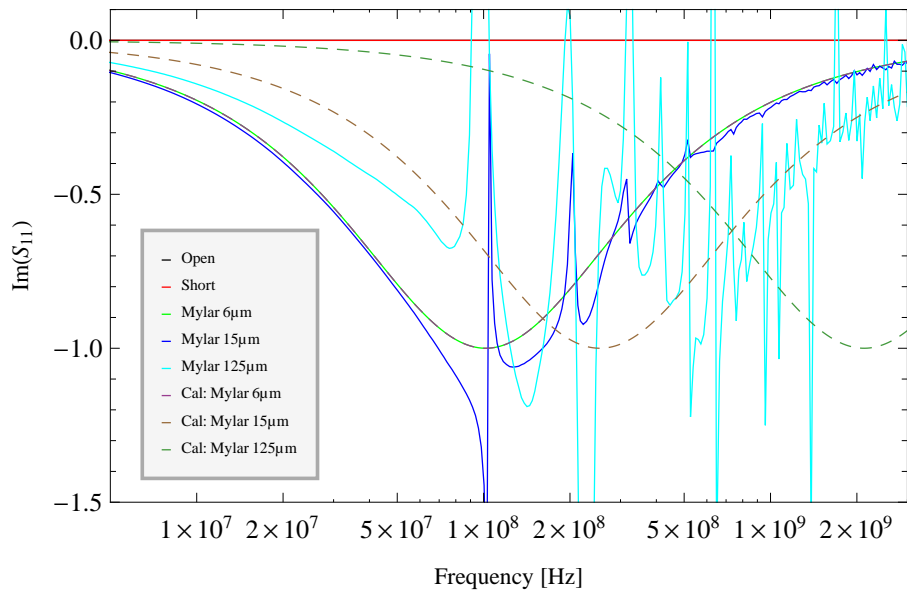


Figure 19: Imaginary part of the corrected data in the frequency range $5 * 10^6 \text{ Hz}$ to $3 * 10^9 \text{ Hz}$ and $|S_{11}| \leq 1$ for a detailed look without irrelevant peaks

3.6 Result

With these corrected S_{11} parameters and (2.10) we can now calculate the relative dielectric constant ϵ_r of our measured samples. We expect ϵ_r to be constant value of $\epsilon_r = 3$.

If we have a look at the ϵ_r we can say that at least the $15\mu m$ sample is almost a constant. The $125\mu m$ sample is a constant until we reach the $100MHz$ mark. The value of the constant is higher then it should be, but that is connected to the shift of the measured S_{11} coefficients. The $15\mu m$ Mylar is increased around the factor $15/6 = 2,5$ to about $7,5$ and the $125\mu m$ sample is increased much higher. The imaginary part isn't shown because it is 0 almost all the time with a few peaks at above $100MHz$.

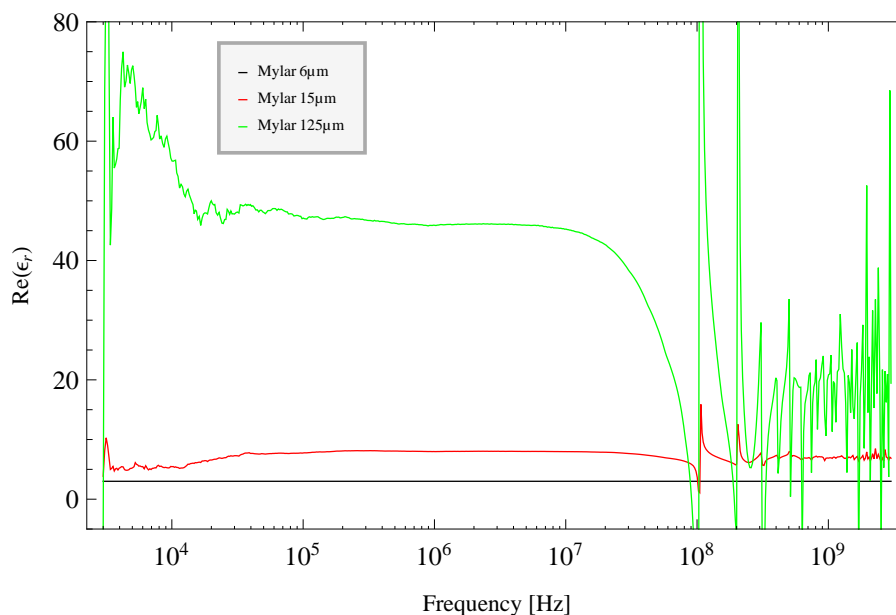


Figure 20: Real part of the dielectric constant

3.7 Checking experiments

Another measurement was made with an analyser from Rohde&Schwarz. We have done the same procedure like with our analyser. The only difference is the frequency range. This measurement is from $10MHz$ to $3GHz$ and we have taken 2001 measuring points. Here we obtain almost the same results as with the other analyser. We can look on the same coincident effect like before.

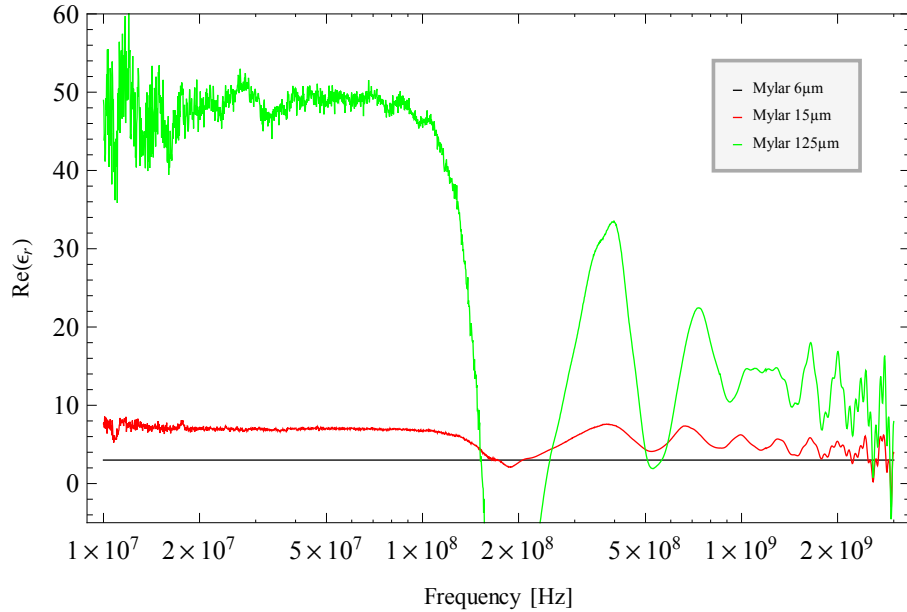


Figure 21: Real part of the dielectric constant in the frequency range $10 * 10^6 Hz$ to $3 * 10^9 Hz$

3.8 Discussion

First of all, it took us some time to perform a correct measurement. At the beginning we have tried to calibrate and measure the whole system (Fig.: 4). We thought that we are measuring an absolute value, a phase and the impedance.

By doing so we have considered the impedance of the transmission line and the sample. We want to consider the impedance of the sample only.

We have also tried to calibrate the $6\mu m$ Mylar as a 50Ω load. There we were able to see that there is a difference between our samples. But we got a reflection coefficient down to -4 ($|S_{11}| \leq 1$).

We have tried to improve our samples by painting them with silver paste. We have done this step to reduce the distance between the sample and the connectors. Because the space between sample and connector is in the area of some $10\mu m$, on both sides. By doing this we measured only short circuited samples.

Finally we have done our calibration in two steps described in the sections 3.2 and 3.3. We have also assured that the network analyser make no mistake with a checking experiment described in section 3.7. The result isn't as we expected but we know that the transmission line causes the errors.

4 FT-IR Measurements

4.1 FT-IR setup

For doing these measurements we have used a Bruker Vertex 80v and the appendant Opus software. How the Bruker works is described in section 2.3. The light path (Fig.: 22) starts at the laser, is focused with an aperture, runs through the Michelson interferometer, is reflected at the probe and than measured with the detector.

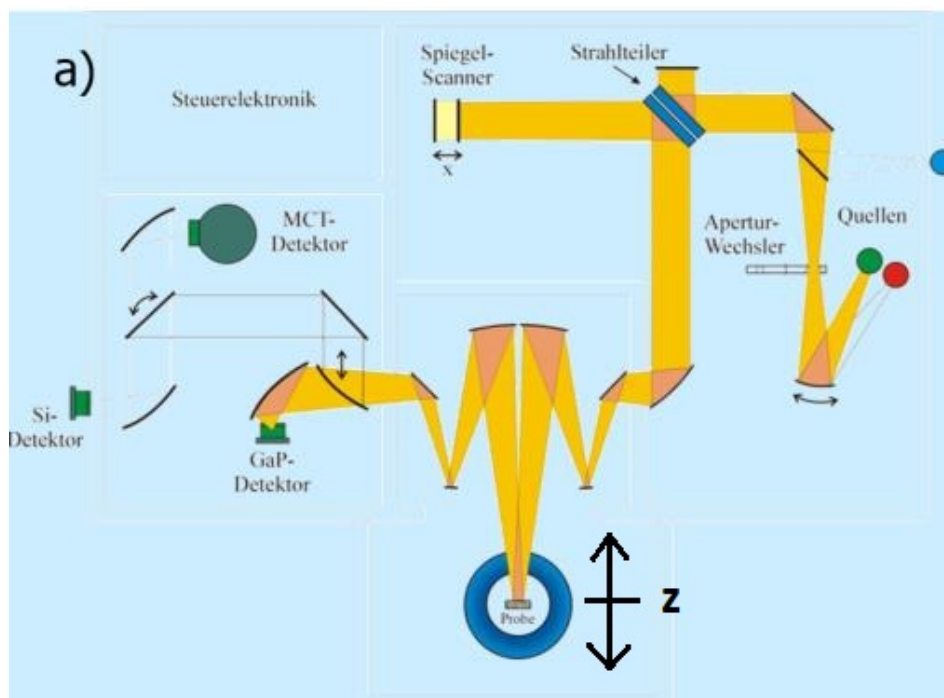


Figure 22: Schematic light path¹

The software is doing the Fourier transformation and gives you the result of the reflection. The whole system is in a vacuum while we do our measurements. In the Bruker we have a pressure of about $1,25hPa$ the whole time. For the resolution we have chosen $1cm^{-1}$, for the phase resolution we have used a value of 8 and for the aperture we have we have chosen $3mm$.

¹Source: http://www.ifp.tuwien.ac.at/fileadmin/Arbeitsgruppen/solid_state_spectroscopy/images/FT1.png

4.2 Calibration

The standard sample holder was too large for our small samples. Thus we had to design and built a custom sample holder to fit on the standard sample holder.

All measurements are reflectivity measurements. As our reference sample we use a gold mirror because a gold mirror has the highest reflection $R = 1$. The whole sample holder can be moved in z-direction (Fig. 22). We have to check at which z-position and aperture we get the highest signal. The highest signal means that the we focus only on the sample and not on the sample and the sample holder.

Because of the disturbance from the components we do not have a reflection $R = 1$ on the whole frequency range. Thus we have to do a background signal measurement with the gold mirror. After doing and applying the background signal we get reflection of $R = 1$ over the whole frequency range.

4.3 Measurement

Then we started with the first reflectivity measurement of MgO. At the MgO data (Fig.: 23) we can observe a peak at a wavenumber of about 400 cm^{-1} and a constant part at higher wavenumbers.

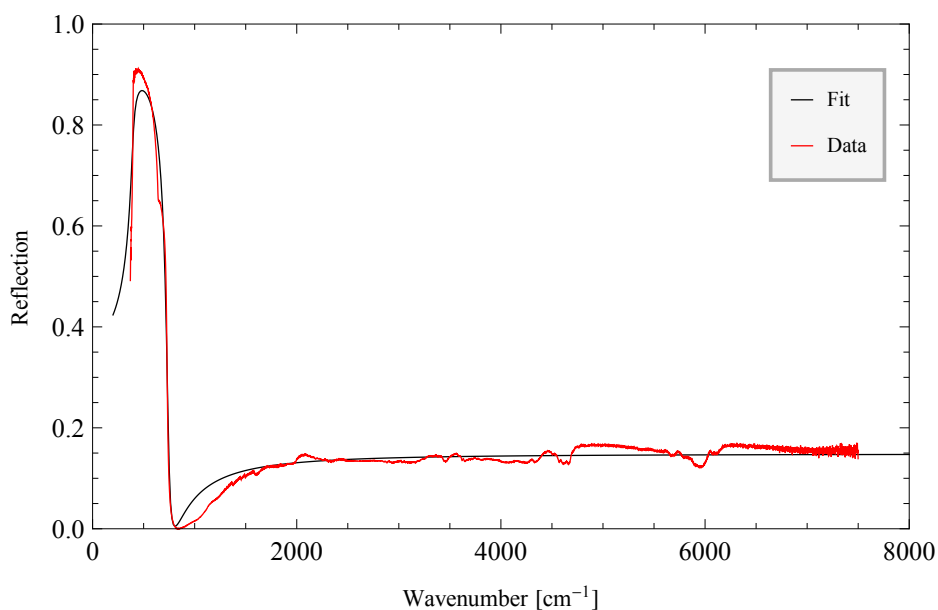


Figure 23: Reflectivity of MgO

Modelling the received data with the program RefFIT we got a fitted dataset (Fig.: 23: Fit) and the values from the program

Maximum	ω_0 cm^{-1}	ω_p cm^{-1}	γ cm^{-1}
1	394,05	1413,86	43,84

Table 1: Fit parameter from MgO

Here we have got a $\epsilon_\infty = 5,07$. This program does a minimisation of the χ^2 and here we got a $\chi^2 = 5,10 * 10^4$. The smaller the value the better it is fitted.

The next sample was NdGaO₃. At the NdGaO₃ data (Fig.: 24) we can observe two high peaks at about a wavenumber of 400 cm^{-1} and 600 cm^{-1} . We can also observe some features above 1600 cm^{-1} which we don't expect. Modelling the

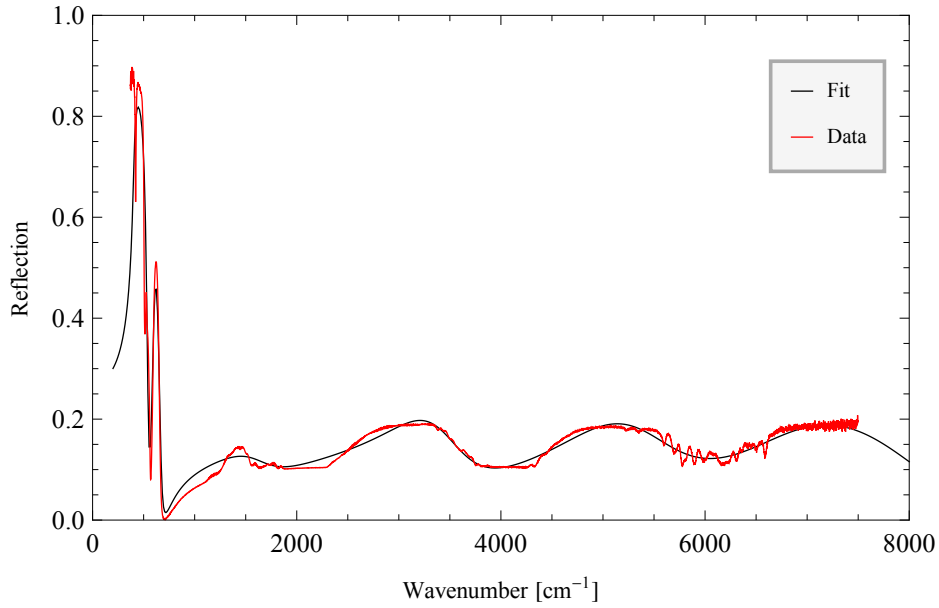


Figure 24: Reflectivity of NdGaO₃

received data from NdGaO₃ with the program ReffIT we got a fitted dataset (Fig.: 24: Fit) and the values from the program

Maximum	ω_0 cm^{-1}	ω_p cm^{-1}	γ cm^{-1}
1	405,72	935,21	28,96
2	593,05	354,54	40,62
3	1601,84	1108,65	677,48
4	3271,26	3048,42	839,45
5	5050,59	4453,16	1290,11
6	6758,71	4718,99	1674,63

Table 2: Fit parameter from NdGaO₃

With an $\epsilon_\infty = 1,69$ and a $\chi^2 = 1,22 \cdot 10^5$. Here we have a worse fit than for MgO. We didn't expect these features (Fig.: 24) above a wavenumber of 1600 cm^{-1} in the reflectance. By using (2.15) for two maxima and subtract one from each other and taking a average distance of 1700 cm^{-1} we obtain a thickness of $\sim 1,5 \mu m$ with a $n = 2$. So we have a second $1,5 \mu m$ thick layer or some effect which behave like a layer with this certain thickness.

5 Discussion and Outlook

Finally we were able to do a serious calibration and to take a measurement from the Mylar samples with the network analyser. If it is a good or a bad one is hard to detect at the first look. But by converting the real and the imaginary part into an amplitude and a phase we saw that something was not perfect. Because the amplitude is dropping so fast and above a high frequency range where we don't expect much absorptions. By checking this phenomena with a second device we got the proof that something is wrong with our device. I think, with more experience with the network analyser it will be easy to find the mistake we made and it will be easy to correct it and it should deliver consistent results. The next phenomena is much more difficult to explain. We think that the calibration measurements and the error parameter calculation is correct, but as figure 20 says, something isn't correct. The good thing is that two different devices deliver the same result (Fig.: 20 and 21). At least the smallest Mylar sample ($15\mu m$) provides an almost constant but shifted result. The calculation should be correct because two different programs deliver the same results. So the only possibility is that the transmission line isn't good enough for these measurements. Instead of Mylar for the calibration a material with an impedance closer to 50Ω will probably make a difference. Furthermore the measurements will be in a cryostat so the calibration needs to be adapted to this case. There is the possibility to make on error coefficient temperature dependent.

In the case of the FT-IT spectrometry all measurements were quite good. Maybe it is interesting to find the second thin layer or to check if the NdGaO_3 sample behaves like there is a thin layer. In the future these measurements will also be performed at low temperatures in a cryostat.

Acknowledgement

First of all I would like to thank Prof. Pimenov for letting me perform this small project at the *Institut für Festkörperphysik der TU Wien* under the guidance of Dr. Johnstone. I would also like to thank Dr. Johnstone for his great guidance in this project. I was glad to have his full support and the possibility to discuss everything with him even if we don't always fully understand each other. Furthermore I would like to thank the members of Prof. Pimenovs group for all their answers to all of my questions.

I also would like to thank the company *x.Test GmbH* for lending us the network analyser and making it possible to do this project. And a thanks to the agent who instructed us to the analyser and answers all our questions.

A special thanks to Ms Geiger who let us perform a measurement on her network analyser and for the great support while doing it.

List of Figures

1	Model of voltage and current at a transmission line	2
2	Two-Port system with wave quantities	3
3	Michelson interferometer[1]	4
4	Schematic measuring setup	7
5	Schematic sample holder geometry	7
6	Real part measurement of the calibration, B: Before and A: After the actual measurement	8
7	Imaginary part measurement of the calibration, B: Before and A: After the actual measurement	9
8	Real part measurement of the transmission line, B: Before and A: After the actual measurement	10
9	Imaginary part measurement of the transmission line, B: Before and A: After the actual measurement	10
10	General error model	11
11	Real part of the measured data	12
12	Detailed real part of the measured data	13
13	Imaginary part of the measured data	13
14	Real part of the calculated error coefficients	14
15	Imaginary part of the calculated error coefficients	15
16	Real part of the corrected data	16
17	Imaginary part of the corrected data	16
18	Real part of the corrected data in the frequency range $5 * 10^6 Hz$ to $3 * 10^9 Hz$ and $ S_{11} \leq 1$ for a detailed look without irrelevant peaks	17
19	Imaginary part of the corrected data in the frequency range $5 * 10^6 Hz$ to $3 * 10^9 Hz$ and $ S_{11} \leq 1$ for a detailed look without irrelevant peaks	17
20	Real part of the dielectric constant	18
21	Real part of the dielectric constant in the frequency range $10 * 10^6 Hz$ to $3 * 10^9 Hz$	19
22	Schematic light path	20
23	Reflectivity of MgO	21
24	Reflectivity of NdGaO ₃	22

References

- [1] M. Dressel and G. Grüner. *Electrodynamics of Solids: Optical Properties of Electrons in Matter*, Cambridge University Press, Cambridge, P. 22, 260ff, (2003).
- [2] K. Lange and K.-H. Löcherer. *Taschenbuch der Hochfrequenztechnik: Grundlagen, Komponenten, Systeme*, Springer - Verlag, Berlin, Heidelberg, P. C17ff, C9ff, (1992).
- [3] W. Demtröder. *Experimentalphysik 2: Elektrizität und Optik*, Springer - Verlag, Berlin, Heidelberg, P. 312f, (2009).
- [4] A. Kuzmenko. Kramers-Kronig constrained variational analysis of optical spectra, *Rev. Sci. Instrum.* 76, 083108 (2005).